Journal of Applied Electrochemistry **29**: 1277–1284, 1999.

Overall mass transfer in the swirling flow induced by a tangential inlet between coaxial cones

M.N. NOUI-MEHIDI[1], A. SALEM[1], P. LEGENTILHOMME[2]* and J. LEGRAND[2]
[1]*Laboratoire de Mécanique des Fluides, Université des Sciences et des Techniques Houari Boumédiène, El-Alia, BP 32, Alger, Algeria;*
[2]*Laboratoire de Génie des Procédés, UPRES EA 1152, Université de Nantes, IUT, CRTT, BP 406, 44602 Saint-Nazaire, France*
*(*author for correspondence; e-mail: legenti@iutsn.univ-nantes.fr)*

Received 16 December 1998; accepted in revised form 16 March 1999

Key words: conical annulus, mass transfer, pressure drop, tangential inlet, visualization

Abstract

An electrochemical method is used to measure mass transfer coefficients between an electrolytic solution and the inner core of a system formed by stationary coaxial cones of the same apex angle. A swirling decaying flow is induced by means of a tangential inlet at the system base. The average mass transfer coefficients are measured at three axial positions from the tangential inlet for both laminar and turbulent flow regimes. Pressure drops between the inlet and the outlet of the experimental device are also investigated. Flow visualization revealed the existence of axially fixed toroidal vortices. The overall mass transfer coefficients along the conical gap are found to be greater than those measured in annular swirling decaying flow for the same values of the annular gap thickness, of the tangential inlet diameter and of the Reynolds number based on the mean axial velocity at the bottom of the conical gap. The enhancement in mass transfer, up to 50% compared with that measured in a cylindrical arrangement, is not counter-balanced by an increase in pressure drop, which remains of the same order of magnitude as that measured in a classical annular configuration.

List of symbols

A	mass transfer surface area (m^2)
A_{co}	gap section of the conical cell (m^2)
A_{cy}	gap section of the cylindrical cell (m^2)
C	bulk concentration of the transferred species (mol m^{-3})
D	diffusion coefficient of the transferred species (m^2 s^{-1})
d	thickness of the Taylor cells in the streamwise direction (m)
e	$= R_{2\max} - R_{1\max}$: gap width (m)
F	Faraday's constant (96 487 C mol^{-1})
I	limiting diffusional current (A)
K	overall mass transfer coefficient (m s^{-1})
L	total length of the cell (m)
L_m	mean axial position of the mass transfer section with respect to the tangential inlet (m)
n	number of electrons involved in the electrochemical reaction
Q	volumic flow-rate (m^3 s^{-1})
Re	Reynolds number ($= 2e\,U_o/\nu$)
$R_{1\max}$	maximum radius of the inner cone (m)
$R_{2\max}$	maximum radius of the outer cone (m)
Sc	Schmidt number ($= \nu/D$)
Sh	Sherwood number ($= 2eK/D$)
Sh_{co}	Sherwood number in the conical arrangement
Sh_{cy}	Sherwood number in the cylindrical arrangement
U_o	mean axial velocity at the base of the cell (m s^{-1})

Greek letters

ΔP	pressure drop (Pa)
ϕ	apex angle of the cones (°)
ϕ_e	diameter of the tangential inlet (m)
λ	friction factor
ν	kinematic viscosity of the working solution (m^2 s^{-1})
θ	inclination of the Taylor cells frontiers with respect to the equatorial plane (°)
ρ	density of the working solution (kg m^{-3})

1. Introduction

Theoretical studies of swirling flows in annular or tubular systems have been the subject of numerous works over more than forty years [1]. These studies have been essentially focused on the hydrodynamic properties of the fluid motion or dedicated to heat and mass transfer enhancement compared with fully developed axial flows. Experimentally, it has been found that swirling flows induce an increase in transfer coefficients

with respect to that obtained in fully developed or developing axial flows often used in industrial processes. Swirling motion can be induced by several means. In cylindrical annular configurations, this type of flow can be obtained by rotating one of the cylinders while axial flow is superimposed [1], or by using one (or several) tangential inlet(s) at the annulus base. The work of Legentilhomme and Legrand [2] has shown that swirling decaying flow induced by means of a single tangential inlet generates overall mass transfer coefficients up to five times greater than those measured at the inner core of an annulus in fully developed axial flow. On the outer cylinder, mass transfer enhancement up to 1000% has been observed by Lefèbvre et al. [3] just downstream of the tangential inlet for short mass transfer sections.

In rotating systems, the use of conical cylinders provides more interesting centrifugal properties than in classical annular configurations. Troschkin [4] has analytically shown that the centrifugal behaviour of the fluid motion between rotating cones increases with apex angle. Bark et al. [5] have studied the motion of two immiscible liquids of different densities in a constant gap between cones both rotating at the same angular velocity. These authors have found that the flow can be divided into two layers: one in which the motion is of the same kind as that of a nonrotating freely falling film, and one in which a kind of rotating-modified Couette–Taylor flow with no net volume flux is observed. Wimmer [6] has studied the stability of the flow between two conical cylinders having the same apex angle, the inner one being rotated at a constant angular velocity and the outer being at rest. He has discussed the hydrodynamic conditions of the appearance of Taylor vortices and spirals between the cones as a function of the variation in the gap ratio.

The present paper describes an experimental study of swirling decaying flow between stationary cones having the same apex angle, the fluid inlet being tangential at the system base. The main purpose of the work is to compare the mass transfer characteristics of this system to those obtained by Legentilhomme et al. [7] between cylinders for the same hydrodynamic and geometric conditions. Pressure drops are also compared with those measured by Lefèbvre et al. [3] in annular swirling decaying flow. Finally, flow visualization has been performed in order to globally characterise the flow-field in such a conical swirling decaying flow. This contribution is an expansion of our previous experimental work on cylindrical swirling decaying flow in conical configurations which, to the authors knowledge, has not been investigated, especially from a mass transfer point of view.

2. Experimental details

The electrochemical cell was formed by two truncated cones of the same apex angle, $\phi = 3°$, and was disposed in such a way that the large base was located at the lower part of the system (Figure 1). The maximum radius of the outer cone was $R_{2\max} = 25$ mm, while that of the inner cone was $R_{1\max} = 18$ mm. The gap width, denoted e, was constant and equal to 7 mm. The height of the fluid column, L, was equal to 395 mm. The outer cone was made in Altuglas while the inner one was machined in PVC. Three nickel electrodes of 10 mm length were fixed on the inner cone surface according to $L_m/(2e) = 0.36$, 6.79 and 21.1, where L_m is the mean axial position of the mass transfer section from the bottom of the cell. The swirl motion was achieved by means of a single tangential inlet at the base of the flow system, such that $\phi_e/e = 1$ (ϕ_e being the diameter of the tangential inlet). This configuration corresponds to a pure swirling decaying flow according to previous work of Legentilhomme and Legrand [2]. The experimental set-up is shown in Figure 2. The electrolyte flowed from a tank through flowmeters and then entered the cell by means of the tangential inlet, before being recycled to the tank via a tangential outlet having the same diameter as that of the

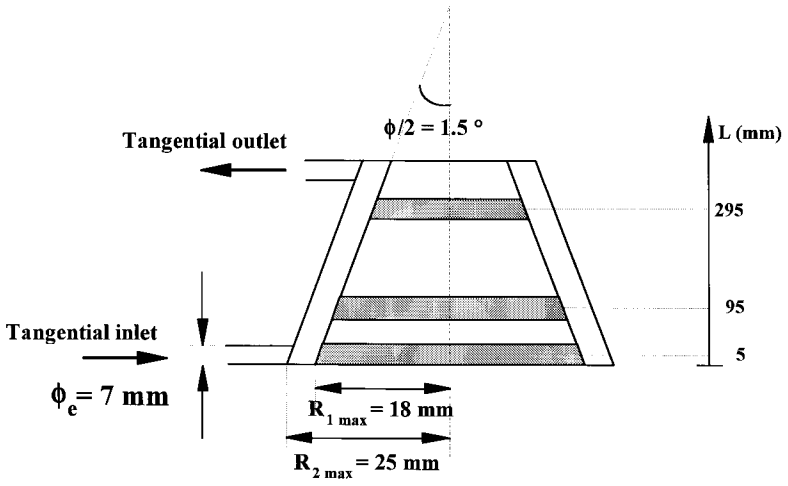

Fig. 1. Sketch of the experimental mass transfer conical cell (not to scale).

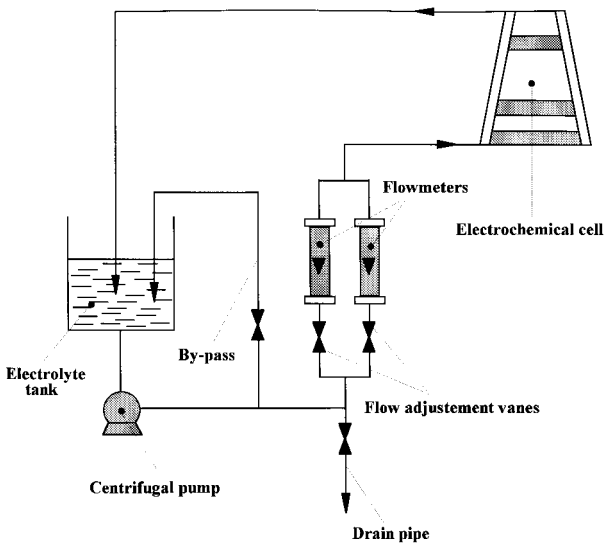

Fig. 2. General view of the experimental facility.

tangential inlet pipe. The fluid temperature was controlled and maintained at a constant value of 30 °C.

Overall mass transfer coefficients on the three electrodes were measured using an electrochemical method. One of the three electrodes acted as anode, whereas mass transfer was measured on the other two acting as cathodes. The electrolyte was an aqueous solution of 2×10^{-3} M potassium ferricyanide, 5×10^{-2} M potassium ferrocyanide and 0.5 M sodium hydroxide. At the constant temperature of 30 °C, the physical properties of the electrolytic solution are given in Table 1. The overall mass transfer coefficient, K, was obtained by means of diffusion controlled reduction of the ferricyanide ions on the working cathodic surfaces and is given by the following equation:

$$K = \frac{I}{nFAC} \tag{1}$$

where I is the limiting diffusion current on the cathode, n is the number of electrons involved in the electrochemical reaction ($n = 1$ for the ferricyanide ion reduction), F is the Faraday constant, A is the cathode surface area, and C is the bulk ferricyanide ion concentration in the solution.

Experimental results are expressed in terms of Sherwood number, Sh, as a function of Reynolds number, Re, respectively defined by

$$Sh = \frac{2eK}{D} \tag{2}$$

Table 1. Physical properties of the electrolytic solution at 30 °C

Property	Value
ρ (kg m^{-3})	1028
v (m^2 s^{-1})	8.73×10^{-7}
D (m^2 s^{-1})	6.95×10^{-10}
$Sc = v/D$	1255

$$Re = \frac{2eU_o}{v} = \frac{2eQ}{v\left[\pi\left(R_{2\max}^2 - R_{1\max}^2\right)\right]} \tag{3}$$

Q being the volumic flow-rate.

Soap and air bubbles were used to observe the main flow structures. Pressure drops between the inlet and the outlet of the experimental device were measured by means of U-manometers using water or mercury. Measurements of overall mass transfer coefficients and pressure drops were made with about 10% accuracy. This uncertainty was evaluated as the maximum difference between repeatability measurements of both pressure drop and mass transfer data and is mainly linked to the flow-rate precision.

3. Results and discussion

3.1. *Flow visualizations*

Figure 3 shows examples of flow visualization in conical swirling decaying flow induced by a tangential inlet. A general helical motion of the fluid occurs which persists up to the top of the conical device (Figure 3(a)) in the investigated range of Reynolds numbers ($500 \leq Re \leq 3500$). This helical motion, noticeable along the entire length of the conical cell, is very interesting compared to flow patterns previously visualized by Aouabed et al. [8, 10] in a cylindrical cell fitted with a tangential inlet. In this last configuration, for small values of the Reynolds number ($100 \leq Re \leq 1500$), the decay in swirl intensity is such that the swirling motion does not persist to the top of the cell (30 cm long in the experimental cylindrical annulus, $e = 7$ mm, of Aouabed et al. [8, 9]). As observed for mass transfer data (Section 3.3.) and previously noted in numerical work [10], the restriction of the conical gap section along the flow path allows the maintenance of a higher tangential velocity component to the top of the conical cell, whereas the fluid motion becomes mainly axial after 20 cm ($L/2e = 14.3$) for Reynolds numbers less than 1500 in cylindrical annular swirling decaying flow [8, 9].

The Taylor-like vortices observed in Figure 3 can be characterised by their streamwise thickness, d, along the flow path. In Figure 4, the reduced thickness of these swirling eddies, $d/2e$, is presented as a function of their mean axial location from the inlet, $L_m/2e$, for several values of Reynolds number. These Taylor-like cells are found to be alternatively thick and thinner along the axis up to the top of the conical gap (Figure 4). These well-defined structures induce a significant enhancement in mass transfer coefficient at the inner cone compared with fully developed axial flow, as previously observed in Taylor–Couette–Poiseuille flow by Coeuret and Legrand [11]. These alternating thick and thinner cells along the flow path can be compared to the flow-field between two concentric cones, the inner one being rotating and the outer at rest, as observed by Wimmer

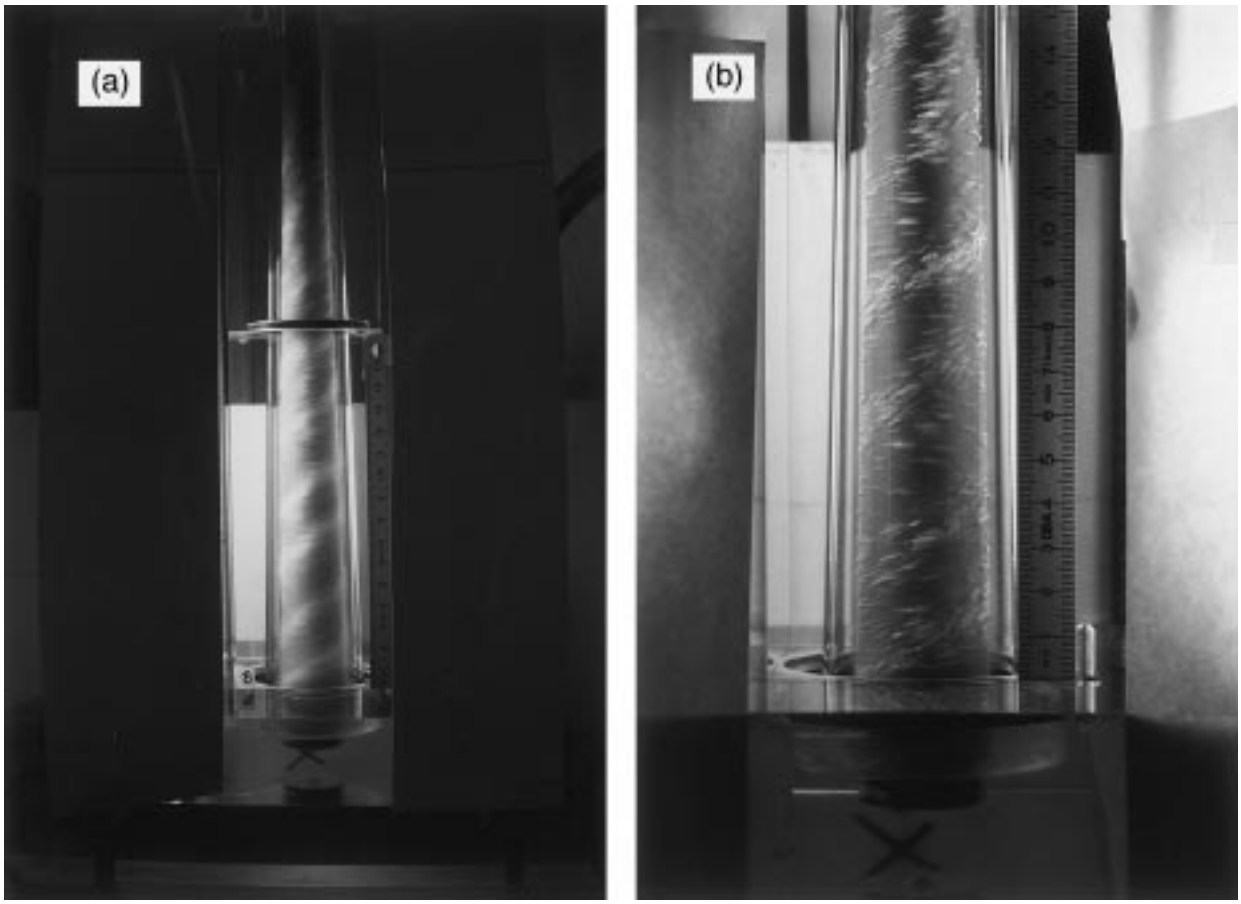

Fig. 3. Examples of flow visualization in conical swirling decaying flow. (a) $Re = 3800$ (soap bubbles); (b) $Re = 1800$ (air bubbles).

[6] in the absence of axial flow. This author noticed that, for each pair of vortices, one of them appears thinner than the neighbouring one. For such a flow, Wimmer [6] has shown that the wavelength, $d/2e$, of a vortex cell is closely linked to its axial position, and that two kinds of vortices can be observed: (i) contra-rotating structures which have an axial length approximately equal to the gap width ($d/2e \cong 0.5$) and (ii) co-rotating vortices having an axial expansion ranged from the gap width to 2.3 times the gap size ($0.5 \leq d/2e \leq 1.15$). In our experimental arrangement, $d/2e$ is almost equal to 2 and does not appear to be linked to the axial distance from the inlet, which means that the axial flow induces a stretching of the vortices compared with that observed by Wimmer [6].

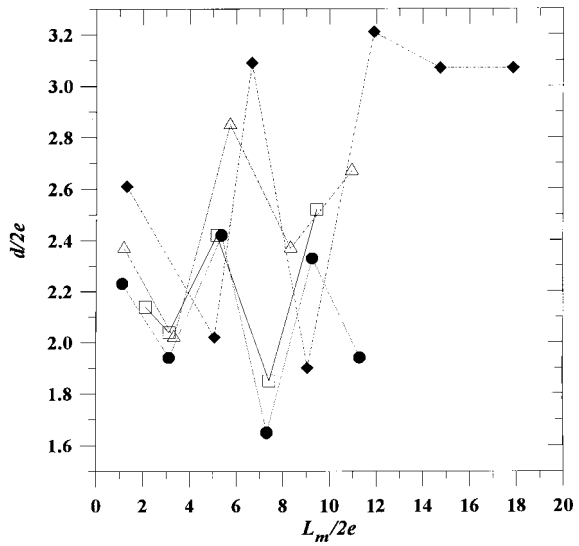

Fig. 4. Variation of the reduced thickness of the Taylor-like vortices, $d/2e$, as a function of the axial distance from the inlet for different values of the Reynolds number. *Re*: (□) 1850, (●) 2900, (△) 3200 and (◆) 3800.

Another interesting feature of these spiral vortices is the angle of inclination, θ, of the cell fronts with respect to the horizontal plane. As observed in Figure 5, this characteristic is not very sensitive to the value of the Reynolds number and remains less than 35 degrees all along the flow path, even at the top of the cell. This fact emphasises the persistant behaviour of the swirling motion in such a conical gap, whatever the value of the Reynolds number in the investigated range ($500 \leq Re \leq 3500$).

3.2. *Pressure drop*

Figure 6 shows a plot of total pressure drop, ΔP, per unit length of the cell, L, as a function of the Reynolds number. The present data dealing with conical swirling decaying flow are compared with those of Lefèbvre et al. [3] in a classical cylindrical configuration having geo-

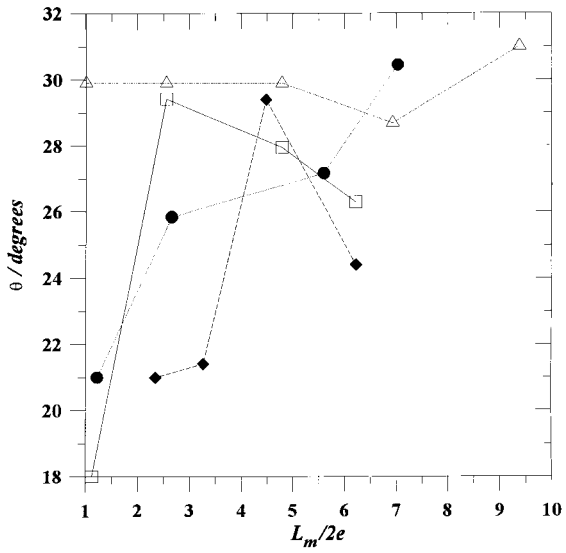

Fig. 5. Influence of the reduced axial location, $L_m/2e$, on the angle of inclination, θ, of the Taylor-like vortices for several Reynolds numbers. *Re*: (□) 540, (●) 1050, (△) 1850 and (◆) 2900.

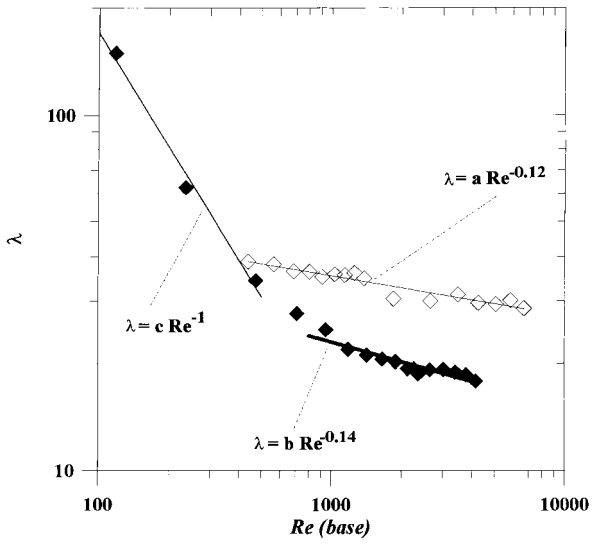

Fig. 7. Friction factor, λ, against *Re*. Comparison with the annular configuration studied by Lefèbvre et al. [3]. Key: (◆) conical system and (◇) cylindrical annulus (Lefèbvre et al. [3]).

metrical characteristics almost identical to that of the conical cell investigated here ($R_{2\max} = 27$ mm, $R_{1\max} = 19$ mm, $\phi_e = R_{2\max} - R_{1\max} = 8$ mm and $L/2e = 50$ mm). In the overlapping range of Reynolds numbers of both experimental works, the total pressure drop, including the contribution of both the tangential inlet and outlet of the cells, is always lower in the conical arrangement in comparison with that measured in the cylindrical one (Figure 6). In fact, the main part of the overall pressure drop is induced by the inlet/outlet system which remains the same in both experimental arrangements.

In Figure 7, the pressure drop measurements are presented in terms of the friction factor, λ, against the Reynolds number. λ is given by the following equation:

$$\lambda = \frac{\Delta P}{\frac{1}{2}\rho U_o^2 \left[\frac{L}{2e}\right]} \tag{4}$$

Two flow regimes can be observed: one for Reynolds number values less than 1000, in which λ is proportional to Re^{-1}, and one for Reynolds numbers greater than 1000, where λ is a slightly decreasing function of *Re*. In the cylindrical configuration (data of Lefèbvre et al. [3]), only the second trend is observed in the whole range of Reynolds numbers investigated ($400 \leq Re \leq 7000$, Figure 7), for which the decrease of λ against *Re* is almost the same as that observed in the second flow regime for the conical arrangement. This different behaviour of the two kinds of swirling decaying flows seems to be due to a delayed transition regime in the cylindrical configuration. This trend is emphasized by the fact that data of Figure 7 are plotted as a function of *Re* based on the bottom dimensions of the conical gap. A plot as a function of *Re* calculated at the mid height of the conical gap will shift the curve λ against *Re* to the right and, consequently, the difference between the two configurations will decrease.

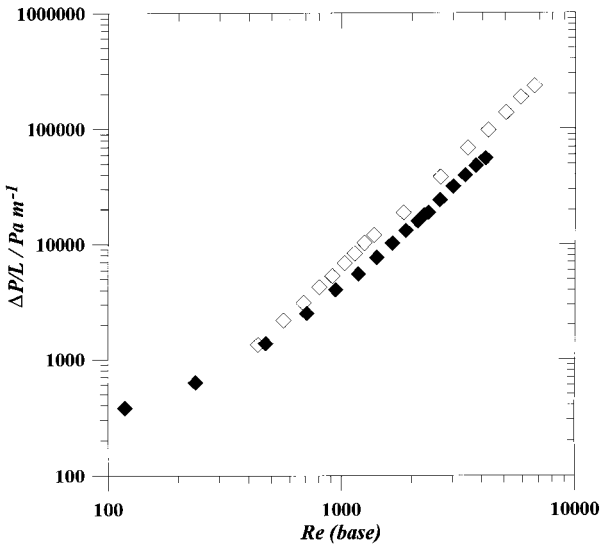

Fig. 6. Evolution of the total pressure drop, $\Delta P/L$, as a function of the Reynolds number. Comparison with the cylindrical swirling decaying flow previously investigated by Lefèbvre et al. [3]. Key: (◆) conical system and (◇) cylindrical annulus (Lefèbvre et al. [3]).

3.3. *Mass transfer data*

Mass transfer measurements in the conical electrochemical cell fitted with a single tangential inlet are plotted in Figure 8 in terms of the overall Sherwood number, *Sh* (Equation 2), against the Reynolds number, *Re*, calculated at the base of the system (Equation 3), for the three investigated axial locations of the mass transfer section, 1 cm long, with respect to the tangential inlet. The overall mass transfer coefficients are found to decrease along the flow path. This general tendency has

been previously observed by Legentilhomme and Legrand [2] and Legentilhomme et al. [7] on the inner cylinder of a classical annular swirling decaying flow induced by a tangential inlet, and by Lefèbvre et al. [3] at the outer core of the same experimental device. As for the commonly used cylindrical geometry, the decay in mass transfer along the flow path in the conical cell is mainly linked to the decrease in swirl intensity downstream of the swirl inducer [2, 3, 7].

In Figure 8, for the three reduced axial positions, $L_m/2e$, of the mass transfer surface, two flow regimes can be distinguished according to the value of the Reynolds number. In laminar flow, for Reynolds numbers between 100 and 1000, the overall Sherwood number is found to vary with *Re* to the power 0.5 as in developing axial laminar flow [12]. In turbulent swirling flow, for Reynolds number values greater than 2000, *Sh* is proportional to $Re^{0.8}$. These two flow regimes observed in Figure 8 have been previously pointed out in swirling annular decaying flow induced by a tangential duct by Legentilhomme and Legrand [2, 13] and Legentilhomme et al. [7]. At the highest axial position ($L_m/2e = 21.1$), a rather constant Sherwood number is measured in both experimental arrangements for Reynolds numbers between 1000 and 3000 (Figure 8). This behaviour, at the top of the cell, may be due to the influence of the tangential outlet which may induce a recirculation zone governing the mass transfer in this range of Reynolds numbers.

In Figure 8, we have also compared the overall mass transfer measured on the second cathode with respect to the tangential inlet, located at a reduced mean axial position, $L_m/2e$, equal to 6.79, in conical and cylindrical [7] configurations to that predicted by Ross and Wragg [14] in fully developed axial flow in laminar and turbulent flow regimes. As in the cylindrical arrangement, mass transfer in conical swirling decaying flow is enhanced in comparison with that obtained in purely axial flow. This fact is due to the incidence of the tangential velocity component, via the swirl intensity, which induces a decrease in the diffusional boundary layer thickness and thus an increase in mass transfer coefficient [2, 7, 13].

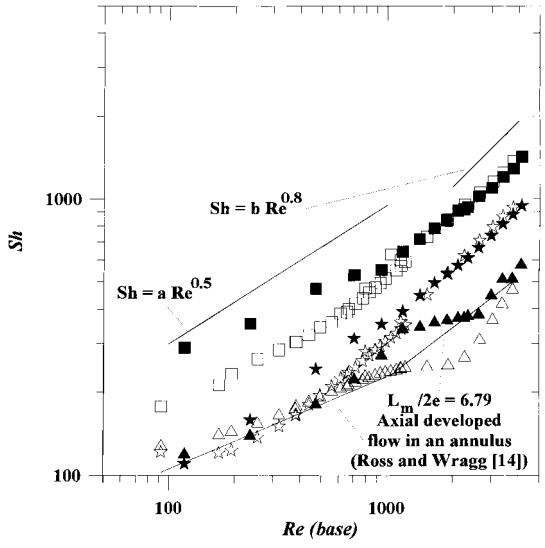

Fig. 8. Mass transfer data against Reynolds number in the conical configuration. Comparison with the experimental results obtained by Legentilhomme et al. [7] in annular swirling decaying flow and with fully developed axial laminar and turbulent flows (after Ross and Wragg [14]). $L_m/2e$ for cylinders (Legentilhomme et al. [7]): (□) 0.36, (☆) 6.79, (△) 21.10; $L_m/2e$ for cones: (■) 0.36, (★) 6.79, (▲) 21.10.

In Figure 8, the present mass transfer data in the conical configuration are also compared to those obtained by Legentilhomme et al. [7] in a cylindrical annular cell having the same basic geometrical characteristics as the conical one ($e = \phi_e = 7$ mm) for the three mean reduced axial positions of the mass transfer section. In laminar flow, for Reynolds numbers less than 1000, mass transfer in the conical device clearly appears greater than that obtained in the classical annular geometry whatever the axial position of the active surface. This is due to an increase in swirl intensity in the conical gap because of a slower decay of the angular velocity component. In a previous numerical study (Noui-Mehidi et al. [10]), we have shown, using a finite-difference method to solve the Navier–Stokes equations by applying the boundary layer theory in the laminar flow regime, that the swirl intensity, defined by the ratio between the angular and axial momentum fluxes [15], is greater and decays more slowly in the conical arrangement than in the annular one. For Reynolds numbers greater than 2000, mass transfer in conical and cylindrical configurations are essentially of the same order of magnitude whatever the axial location of the mass transfer surface (Figure 8). As previously noticed by Legentilhomme et al. [7] in annular geometry, the increase in Reynolds number induces a swirling motion which persists higher in the cell than in the laminar swirling flow regime. Thus the tangential velocity component is significant all along the annulus and, in this case, the increase in axial velocity in the conical geometry with the axial distance has no significant effect on the swirl motion. Consequently, the mass transfer in this range of Reynolds numbers is mainly controlled by the tangential velocity component. Furthermore, the decay in mass transfer along the flow path seems to be of the same type, especially in turbulent flow (Figure 8), in the two tested configurations.

In their previous study, Lefèbvre et al. [3] have established an energetic correlation linking the overall mass transfer measured on both cylinders of their annular cell, for mass transfer section lengths between 0.1 and 0.4 m, to the pressure drop in the cell. These authors have shown that the swirling annular decaying flow induced by a single tangential inlet equal in diameter to the annular gap thickness is very promising from an energetic point of view. For instance, this type of flow appears more interesting than the well-known fully developed axial flow, and even more efficient than the swirling annular decaying flow generated by helical

inserts at the entrance of the system investigated by Yapici et al. [16, 17]. Looking at experimental data presented in Figures 8 and 6, respectively concerned with overall mass transfer and pressure drop, it can be argued that conical swirling decaying flow is more interesting than classical annular flow from an energy consumption point of view.

Figure 9 shows the ratio between the Sherwood number in conical, Sh_{co}, and cylindrical, Sh_{cy}, swirling decaying flows as a function of the Reynolds number for the three positions, $L_m/2e$, of the mass transfer section. In this Figure, Sh_{co}/Sh_{cy} is compared with the ratio A_{cy}/A_{co} between the gap section areas, at each corresponding mean axial location, $L_m/2e$, of the cylindrical, A_{cy}, and the conical, A_{co}, geometries. For the lowest axial position of the mass transfer section ($L_m/2e = 0.36$), the ratio Sh_{co}/Sh_{cy} is greater than A_{cy}/A_{co} in the investigated range of Reynolds numbers and taking into account the accuracy of the mass transfer data. For small values of *Re*, a recirculating eddy appears on the inner core of the cylindrical configuration (Farias Neto et al. [18]). This flow pattern, which is not observed in the conical arrangement, induces a rather low mass transfer on the first cathode. As the Reynolds number is increased, enhancing the swirling motion of the fluid just downstream of the tangential inlet, mass transfer in both geometries becomes controlled by the tangential velocity component and thus the ratio Sh_{co}/Sh_{cy} tends towards unity (Figure 9). Therefore, for this lowest position of the mass transfer section, for small Reynolds numbers, the section restriction along the conical device is not sufficient to explain the enhancement of mass transfer compared with the cylindrical configuration. For the two highest cathodes ($L_m/2e = 6.79$ and 21.1), the ratio Sh_{co}/Sh_{cy} does not decrease monotonically with *Re* (Figure 9). For Reynolds numbers between 100 and 1000, this ratio first increases to reach a maximum value and thereafter decreases towards unity for *Re* varying between 1000 and 4000. In the first range of Reynolds numbers, the recirculation zone previously discussed develops to progressively reach the intermediate transfer section ($L_m/2e = 6.79$) on which mass transfer in the cylindrical arrangement is rather independent of *Re*, whereas in the conical geometry mass transfer is controlled by the swirling motion. Thus, the ratio Sh_{co}/Sh_{cy} increases with *Re* to reach a maximum value. As for the lowest cathode, a further increase in Reynolds number induces a higher swirl intensity in the cylindrical annulus for which mass transfer also becomes governed by the tangential velocity component. Consequently, the ratio Sh_{co}/Sh_{cy} decreases towards unity. The same behaviour is observed for the highest mass transfer section ($L_m/2e = 21.10$), the peak value of Sh_{co}/Sh_{cy} being shifted to higher Reynolds numbers, because the recirculation zone reaches the top of the cell for higher Re in the cylindrical arrangement (Farias Neto et al. [18]). Furthermore, for the highest cathode, Sh_{co}/Sh_{cy} always remains smaller than A_{cy}/A_{co} due to end effects of the tangential outlet (7 mm in diameter for both arrangements), which may be more sensitive in the conical configuration smaller in end cross-sectional area than the cylindrical one.

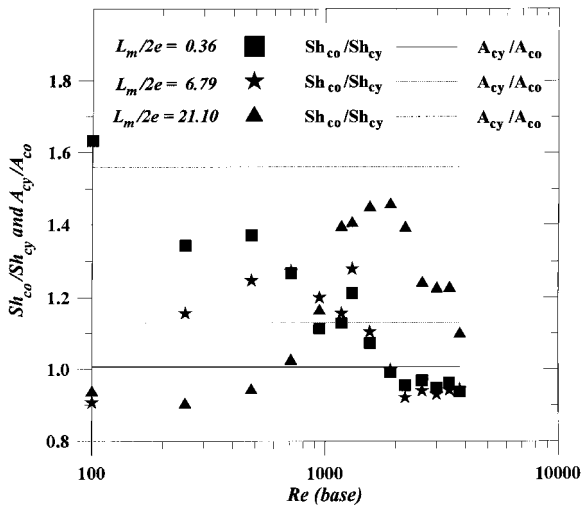

Fig. 9. Evolution of the ratio Sh_{co}/Sh_{cy} between the Sherwood numbers in conical, Sh_{co}, and cylindrical, Sh_{cy}, configurations as a function of Reynolds number for the three axial reduced positions of the mass transfer section. Comparison with the ratio A_{cy}/A_{co} of the cylindrical, A_{cy}, and conical, A_{co}, gap sections.

4. Conclusion

Overall mass transfer coefficients on 1 cm long sections of the inner cone, obtained by means of the well-known electrochemical method involving the reduction of the ferricyanide ions, have been found to be greater than those measured in a more classical annular cell fitted with a tangential inlet equal in diameter to the cylindrical gap width. This enhancement in mass transfer, up to 30% for some hydrodynamic conditions, occurs up to the top of the conical cell, and is mainly due to a swirling motion which persists higher in the cell than in the cylindrical configuration. These stronger and more persistent swirling characteristics can be attributed to the restriction of the cross-sectional area of the conical gap along the flow path, but are also linked to different flow behaviour in the two types of swirling decaying flow. Indeed, in the conical gap, spiral vortices can be observed up to the top of the cell, whereas vortex structures have only been detected at the bottom of the annular cell and which rapidly decay along the flow path. Thus, the continuous reduction of the gap cross-section, which induces an increase in the resulting mean velocity, allows a persistent tangential motion and stable rolling cells along the entire length of the cell.

The enhancement in overall mass transfer in conical swirling decaying flow is not counter-balanced by an increase in pressure drop in comparison with the cylindrical arrangement. Thus, conical swirling flow induced by means of a tangential inlet is very promising from an energy consumption point of view.

References

1. L. Talblot, *J. Appl. Mech.* **21** (1954) 1.
2. P. Legentilhomme and J. Legrand, *Int. J. Heat Mass Transf.* **34** (1991) 1281.
3. G. Lefèbvre, S.R. Farias-Neto, H. Aouabed, P. Legentilhomme and J. Legrand, *Can. J. Chem. Eng.* **76** (1998) 1039 (in French).
4. O.A. Troshkin, *Teor. Osnovny Khim. Tekhnol.* **7** (1973) 897.
5. F.H. Bark, A.V. Johanson and C.G. Carlson, *J. Méc. Théori. Appli.* **3** (1984) 861.
6. M. Wimmer, *J. Fluid Mech.* **292** (1995) 205.
7. P. Legentilhomme, H. Aouabed and J. Legrand, *Chem. Eng. J.* **52** (1993) 137.
8. H. Aouabed, P. Legentilhomme, C. Nouar and J. Legrand, *J. Appl. Electrochem.* **24** (1994) 619.
9. H. Aouabed, P. Legentilhomme and J. Legrand, *Exp. Fluids* **19** (1995) 43.
10. M.N. Noui-Mehidi, A. Salem, P. Legentilhomme and J. Legrand, *Int. J. Heat Fluid Flow* (1999) in press.
11. F. Coeuret and J. Legrand, *Electrochim. Acta* **26** (1981) 865.
12. F. Coeuret and A. Storck, 'Eléments de Génie Electrochimique' (Lavoisier, Paris, 1984).
13. P. Legentilhomme and J. Legrand, *J. Appl. Electrochem.* **20** (1990) 216.
14. T.K. Ross and A.A. Wragg, *Electrochim. Acta* **10** (1965) 1093.
15. A.K. Gupta, D.G. Liley and N. Syred, 'Swirl Flows' (Abacus Press, Cambridge, 1984).
16. S. Yapici, M.A. Patrick and A.A. Wragg, *Int. Com. Heat Mass Transf.* **21** (1994) 41.
17. S. Yapici, G. Yapici, C. Özmetin, H. Ersahan and Ö çomakly, *Int. J. Heat Mass Transf.* **40** (1997) 2775.
18. S.R. Farias Neto, P. Legentilhomme and J. Legrand, *Comp. Meth. Appl. Mech. Eng.* **165** (1998) 189.